



Comparison of NO_x and PN emissions between Euro 6 petrol and diesel passenger cars under real-world driving conditions



Jianbing Gao^{a,b,*}, Haibo Chen^b, Ye Liu^b, Juhani Laurikko^c, Ying Li^d, Tiezhu Li^e, Ran Tu^e

^a School of Mechanical Engineering, Beijing Institute of Technology, Beijing 100081, China

^b Institute for Transport Studies, University of Leeds, Leeds LS2 9JT, UK

^c Engine and Vehicle Emissions, VTT, 02044 VTT, Finland

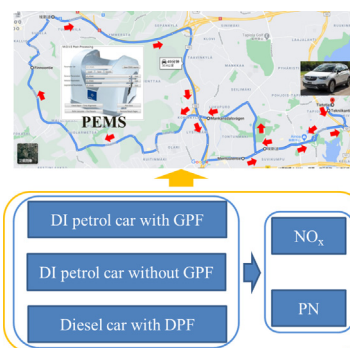
^d Dynnoteq, 61 Bridge Street, Kington HR5 3DJ, UK

^e School of Transportation, Southeast University, Nanjing 210009, China

HIGHLIGHTS

- NO_x and PN emissions of Euro 6 passenger cars are tested under real-world conditions.
- Comparisons in NO_x and PN emissions for petrol and diesel cars are made.
- Significant high NO_x and PN concentrations are observed in petrol passenger cars.
- Relationships between NO_x and PN emission factors and driving behaviours are analysed.

GRAPHICAL ABSTRACT



ARTICLE INFO

Article history:

Received 22 June 2021

Received in revised form 19 July 2021

Accepted 16 August 2021

Available online 21 August 2021

Editor: Kassomenos Pavlos

Keywords:

Real-world driving
Particulate number
Nitrogen oxides
Petrol passenger cars
Diesel passenger cars

ABSTRACT

With emission standards becoming stricter, nitrogen oxides (NO_x) and particle number (PN) emissions are the main concerns of modern passenger cars, especially for the real-world driving. In this paper, two direct injection (DI) petrol passenger cars and a diesel passenger car are tested on the same routes, driven by the same driver. Instantaneous NO_x and PN emissions are monitored by a portable emission measurement system (PEMS) in the tests. During the real-world driving, the exhaust temperatures of the two petrol cars are sufficiently high to ensure high efficiency of three-way catalysts (TWCs). On the other hand, the exhaust temperatures of the diesel car in some sections of the route are lower than the crucial light-off temperature of the selective catalytic reduction (SCR) below which its effectiveness in NO_x reduction would be much affected. NO_x and PN concentrations are low during motorway driving for the petrol passenger car equipped with a gasoline particulate filter (GPF); however, they are high and change frequently in the whole journey for the petrol passenger car without a GPF. NO_x emission factors are quite low over most of the driving sections for the diesel car, but some significant high peaks are observed in the acceleration process. NO_x emission distributions over speed and acceleration are similar for both petrol cars; and they differ significantly from the diesel counterpart. Particle size from the diesel car is the largest, followed by the petrol car with a GPF.

© 2021 Published by Elsevier B.V.

* Corresponding author at: School of Mechanical Engineering, Beijing Institute of Technology, Beijing 100081, China.

E-mail addresses: redonggaojianbing@163.com (J. Gao), H.Chen@leeds.ac.uk (H. Chen), y.liu8@leeds.ac.uk (Y. Liu), juhani.laurikko@vtt.fi (J. Laurikko), litiezhu@seu.edu.cn (T. Li), turancoalg@seu.edu.cn (R. Tu).

1. Introduction

Road transport sector is one of the big contributions to air pollution (Costagliola et al., 2018; Gao et al., 2022). According to the UK government report (Emissions of air pollutants in the UK) published in 2019, particles smaller than 10 μm (PM_{10}), particles smaller than 2.5 μm ($\text{PM}_{2.5}$), and NO_x emissions from road transport account for approximately 12%, 13%, and 33% of the country's total emissions respectively. Advanced techniques are adopted to achieve the downsizing of internal combustion engines such as turbochargers (Lee et al., 2016), which results in high in-cylinder combustion temperature, contributing to the formations of more fine particles and nitrogen oxides (NO_x) emissions (Prasath et al., 2020). However, fine particles have greater harm to human health and the environment than coarse particles (Lelieveld and Pöschl, 2017; Tobias et al., 2018) due to their deeper penetration into the respiratory system. In order to reduce exhaust emissions from on-road vehicles, strict emission standards are set such that emission factors from on-road vehicles are lower than the limits derived from the standard driving cycles (Tutuianu et al., 2015). However, emission factors vary substantially from cycle to cycle (Bielaczyc et al., 2016; Demuynck et al., 2012; Karjalainen et al., 2014; Ko et al., 2017). It was demonstrated by (Marotta et al., 2015), NO_x emission factors over the Worldwide harmonized Light vehicles Test Cycles (WLTC) were much higher than the New European Driving Cycle (NEDC), and the factors over WLTC were eight times of the factors over NEDC for the maximum difference. Hu et al. (Hu et al., 2021) investigated the impacts of driving cycles on particle mass (PM), particle number (PN), and particle size distributions of three direct injection (DI) petrol cars, with one being equipped with a gasoline particulate filter (GPF). For the car with a GPF, PN emission factors were more dependent on the driving cycles than the ones without GPFs (Hu et al., 2021). In reality, real-world driving conditions are much more complex than the standard driving cycles. WLTC is closer to real-world driving conditions than NEDC, but NO_x and particle emissions over WLTC are still much lower than real-world driving (Merkisz et al., 2016).

Real-world driving emission (RDE) test procedures are introduced into Euro-6 emission standards to limit real-world emissions (Giechaskiel et al., 2019; Hooftman et al., 2018), especially for NO_x and particle emissions. Euro-6 emission standard limits both PM and PN emissions from DI petrol cars (Weber et al., 2019; Yinhui et al., 2016). In order to meet the strict emission standard on particles, GPFs are usually applied to DI petrol cars (Awad et al., 2020; Jang et al., 2018; McCaffery et al., 2020; Yang et al., 2018); GPFs present excellent performance of PM and PN emission reductions, especially for solid phase particles (Baek et al., 2020; Chan et al., 2016; Jang et al., 2018). Due to the different driving behavior over various driving cycles, the efficiency changed significantly from cycle to cycle (Jang et al., 2018). The filter efficiency of GPFs is approximately 86.2%, 96.1%, and 77.3% for the driving cycles of Federal Test Procedure (FTP-75), WLTC, and Supplemental Federal Test Procedure (US06) respectively. The Regarding diesel passenger cars, DPFs as the most successful technique controlling PM and PN emissions are widely used, and their performances over various driving cycles have been researched (Bermúdez et al., 2014; Hays et al., 2017; Hoepfner and Roduner, 2013; Li et al., 2013). The filter efficiency of DPF was in the range of 82–95% over the driving cycle of WLTC, NEDC, and extra urban driving cycle (EUDC).

It was demonstrated by Demuynck et al. (Demuynck et al., 2017), PN emission factors from a DI petrol car without a GPF were below the standard limits over WLTC; however, the factors were increased to three times of PN limits under real-world driving conditions. With the introduction of a GPF, PN emissions were dropped to a low level meeting the emission standard under real-world driving conditions. Real-world PN emission factors were also demonstrated to be much higher than lab tests based on standard driving cycles (Wihersaari et al., 2020). Ko et al. (Ko et al., 2019) researched the real-world PN emissions from a DI petrol car equipped with a GPF, and indicated that the cold

start phase contributed to more than 70% of the total PN emissions, implying the large contributions from liquid phase particles. In the cold start phase, PN concentration was much higher than other conditions, and majorities of the particle size were smaller than 150 nm. Particles with size being smaller than 23 nm were more than 60% of the total PN emissions (Ko et al., 2019).

NO_x emission rates of diesel passenger cars over real-world driving were much higher than those from WLTC and NEDC conditions (Triantafyllopoulos et al., 2019), especially under cold start conditions (Gao et al., 2019a; Gao et al., 2019b). The NO_x emissions over real-world driving were approximately twice of the values over WLTC, and almost 10 times of NEDC (Triantafyllopoulos et al., 2019). It also addressed the importance of the real-world emission monitor and indicated the NO_x contributions from cold start stages; additionally, the variations of real-world NO_x emissions were significant for petrol passenger cars (Valverde et al., 2019). Cha et al. (Cha et al., 2019) showed that NO_x emission factors over real-world driving conditions were approximately seven times of the emission limits based on 17 Euro-6 compliant passenger cars. O'Driscoll et al. (O'Driscoll et al., 2018) compared NO_x emissions from diesel and petrol passenger cars under real-world driving conditions, showing that NO_x emission factors of diesel cars were much higher than petrol cars, especially on motorways, mainly due to more NO_x formations and lower efficiency of the NO_x reduction system.

In summary, there are many real-world tests being conducted for passenger cars, and the real-world emissions are compared over various driving cycles in labs. However, the real-world emission comparisons e.g. NO_x and PN from DI petrol cars and diesel cars which meet Euro-6 emission standards over the same routes and same driver are still under-studied. Previous published results include the impacts from driving habits which present significant effects on emissions (Böttcher and Müller, 2015; Hasan et al., 2019). In this paper, two DI petrol cars and a diesel car are tested under real-world driving conditions. A portable emission measurement system (PEMS) is used to monitor instantaneous NO_x and PN emissions. The comparisons of the emissions from these three passenger cars are made; meantime, the distributions of the average emission rates over speed and acceleration are analysed. This research makes the foundations of the future focuses on dropping real-world emissions from passenger cars.

2. Experimental section

2.1. Vehicle information

The specifications of the three passenger cars are given in Table 1. There are two petrol cars and a diesel car; they meet Euro-6 emission standards. For the two petrol cars, three-way-catalysts (TWCs) are used to control the gaseous emissions; one of them is equipped with a GPF to control the particle emissions. Regarding the diesel passenger car, a diesel oxidation catalyst (DOC), a DPF and a SCR are used to control both gaseous and particle emissions. All the passenger cars are turbocharged and direct fuel injection, and P-GPF has the smallest engine size. Because of the direct injection applications, particle formations of petrol cars are increased significantly, resulting from the rich air/fuel zones due to short fuel diffusion process. It should be noted that the compression ratio of P-N-GPF is much higher than the other petrol passenger car. Generally, high compression ratio will lead to high in-cylinder combustion temperature, with the results of more and finer particles; additionally, P-N-GPF is free of a particle filter which may result in high PN emissions.

2.2. Test equipment and procedure

NO_x and particle emission factors are significantly affected by cold start events in the journey (Merkisz et al., 2019); such that the cold start events will affect the analysis of the relationships between

Table 1
Vehicle specifications of the test vehicles.

Car label	P-GPF	P-N-GPF	D-DPF
Car maker	Opel	Skoda	Skoda
Model	Crossland-X	Octavia	Octavia
Manufacture year	2019	2017	2019
Fuel type	Petrol	Petrol	Diesel
Fuel delivery	Direct injection	Direct injection	Direct injection
Aspiration	Turbocharged	Turbocharged	Turbocharged
Engine size/ L	1.12	1.5	1.6
Max. power @ speed/ kW @RPM	81@5500	110@5000	85@3250-4000
Max. torque @ speed/ Nm @RPM	125@1500	250@1500-3000	250@1500-3000
Compression ratio	10.5	12.5	16.2
Running mass/ kg	1278	1470	1556
After-treatment	Gaseous TWC Particles GPF	TWC -	DOC + SCR DPF
Emission standards	Euro-6d_temp	Euro-6c	Euro-6d_temp
Gear number (type)	6 (A)	6 (M)	7 (DSG)
Type approval cycle	WLTP	WLTP	WLTP
Type approval NO _x (mg/km)	17.5	34.1	29.2
Type approval PN (#*10 ¹¹)	4.2	1.08	0.02
Type approval CO ₂ (g/km)	153	115	141
Mileage/km	34,261	73,494	31,204

emission factors and driving behaviours (Gao et al., 2021). Real-world NO_x and PN emissions of the three passenger cars were monitored using a state-of-the-art gas PEMS and a particle PEMS. The specifications of the gas PEMS and particle PEMS are shown in Table 2 and Table 3 respectively. This system included a gas module and a particle module which accurately measured the concentration of NO_x and PN emissions from both petrol and diesel cars. An ultraviolet (UV) analyser was used to measure NO_x concentration. Total particles included solid phase and liquid phase particles, and only the particles being larger than 23 nm were counted by the PEMS system. In order to avoid the effect from high-volatility substances and water vapors, the thermal denuder was heated to 300 °C. PEMS was installed at the back of the cars and an extension to the exhaust tailpipe was used to mount an exhaust flow meter (EFM) tube along with a temperature sensor used to monitor the exhaust flow rates and temperature, as well as a sampling probe at the very end. Fig. 1 shows the real-world driving routes and test cars. The PEMS was calibrated before the test, and the cars were fully warmed up (coolant temperature being approximately 70 °C) before the test run to avoid the cold impacts. AVL Concerto M.O.V.E post processing program was used to record the sampling data, including gaseous pollutants, PN. Longitude, latitude, and altitude were also

Table 2
Specifications of the particle PEMS.

Items	Value
Maker	AVL
Operating temperature	-30 to 45 °C
Storage temperature	-40 to 70 °C
Weight	50 kg
Warm-up time at 20 °C ambient temperature	<1 h
Sample flow rate	3.5 L/min
Measurement range	HC: 0-30,000 ppm NO: 0-5000 ppm NO ₂ : 0-2500 ppm CO: 0-5 v.% CO ₂ : 0-20 v.%
Zero drift	HC: <15 ppm/8 h NO: 2 ppm/8 h NO ₂ : 2 ppm/8 h CO: 20 ppm/8 h CO ₂ : 0.1 v.%/8 h

Table 3
Specifications of the particle PEMS.

Items	Value
Maker	AVL
Operating temperature	5 to 40 °C
Storage temperature	-40 to 70 °C
Weight	45 kg
Warm-up time at 20 °C ambient temperature	<0.5 h
Data logging frequency	1 Hz standard, 5 Hz for selected values
Dilution ratio (constant)	up to 20
Sample flow over filter	6 L/min
Soot measuring range	up to 1000 mg/m ³ (at dilution ratio 20)
Soot detection limit	~5 µg/m ³

recorded by a GPS system. All second-by second data was saved into a laptop. In this paper, the analysis is only focused on NO_x and PN emissions which are the main concerns of the modern passenger cars.

The three vehicles were driven by the same driver on the same routes. The route started from the VTT research centre (Finland), including rural roads, urban roads, and motorways. The percentages of the urban roads, rural roads, and motorways in the total distance were around 76.8%, 16.5%, and 6.7% respectively; the speed limitations were marked in the map as well. The altitude along the driving distance during the journey is shown in Fig. 2. As can be seen, the changes of the altitude over the routes were gentle.

3. Results

In this section, the test results are presented and the comparisons of the real-world driving emissions among the three passenger cars are conducted; meantime, the relationships between exhaust emission rates (e.g. NO_x and PN) and driving behaviours (e.g. speed and acceleration) are analysed.

3.1. Emissions under real-world driving conditions

Real-world driving parameters of P-GPF including speed, acceleration, and exhaust temperature are shown in Fig. 3. The videos during the real-world driving were also recorded to check the driving situations for data analysis. The snapshots of the video during the car running are shown in Table S1. At the first half period of the journey, the speed was lower than 60 km/h during most of the driving time. There were several sections where the speed approached to zero due to the traffic lights. During the first half period of driving, acceleration changed significantly due to the frequent acceleration and deceleration events; additionally, the exhaust temperature was in the range of 500- 650 °C. After the rural and urban driving, the car was driven on the motorways where the speed was increased to nearly 100 km/h from 40 km/h in a short time, and the exhaust temperature was increased up to 800 °C. The exhaust temperature was decreased gradually after a short period of the motorway driving due to low acceleration. During the motorway driving, the acceleration was low. Then, the car was driven on the ring roads from the motorways, followed by a sudden decrease and an increase of speed. The speed was kept at around 85 km/h. After the ring roads, the speed varied in the range of 0- 55 km/h with frequent deceleration and acceleration. Huang et al. (Huang et al., 2019) monitored the exhaust temperature of a petrol passenger car, and the monitoring point was at the end of tail-pipe where the exhaust temperature was lower than 130 °C.

Fig. 4 presents the concentration of NO_x and PN emissions in the real-world driving tests. NO_x concentration changed significantly on the rural roads and urban roads, where the exhaust temperature was



Fig. 1. Real-world driving routes and test cars.

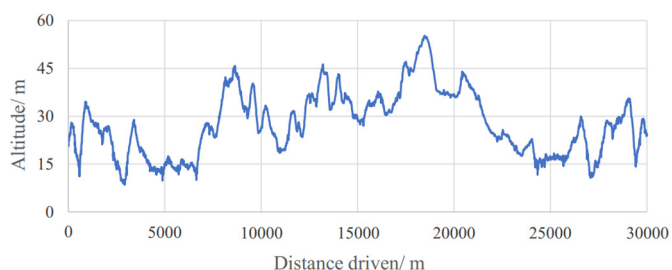


Fig. 2. Altitude along the driving distance.

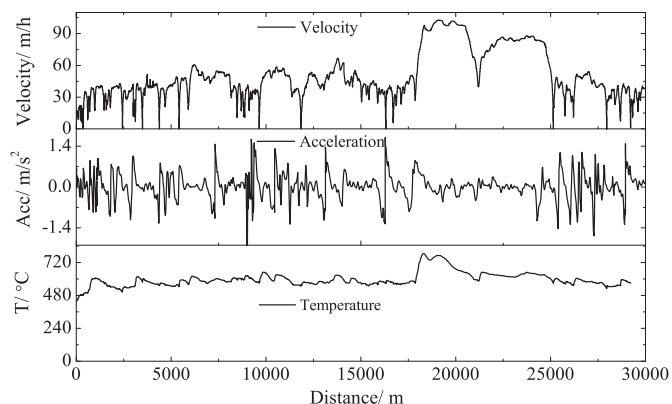


Fig. 3. P-GPF real-world driving parameters.

higher than 500 °C which ensured high TWC efficiency. The variations of pipe-out NO_x concentration were affected by exhaust flow rates and engine-out concentration in theory. In the motorway driving process, NO_x emission concentration was quite low, being benefited from high exhaust temperature and low variations of the vehicle acceleration (low engine-out concentration). PN concentration was low over motorway driving. Seen from the figures, frequent acceleration and deceleration led to more NO_x and PN emissions. Highest PN concentration was observed under low speed and positive acceleration conditions for a DI petrol car (McCaffery et al., 2020), which agreed with the authors' work. Yang et al. (Yang et al., 2019) demonstrated the relationships between PN concentration and exhaust temperature, the peaks of PN concentration usually corresponded to low temperature events. In the

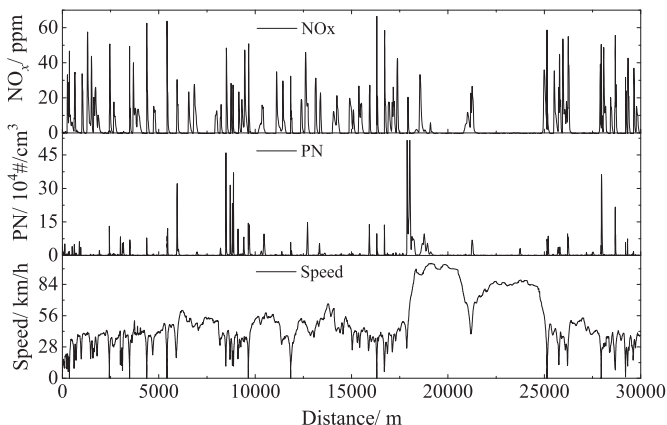


Fig. 4. P-GPF emissions over real-world driving conditions.

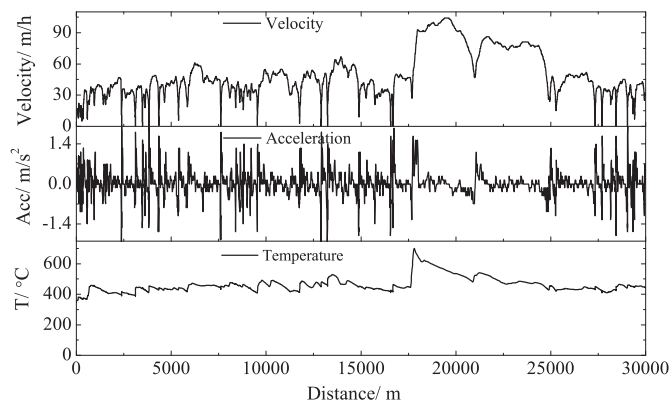


Fig. 5. P-N-GPF real-world driving conditions.

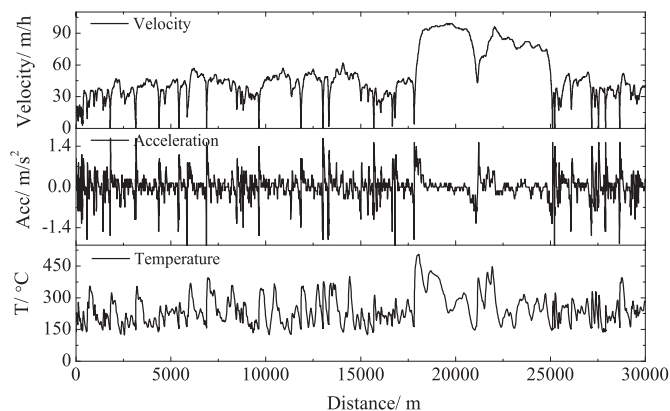


Fig. 7. D-DPF real-world driving parameters.

authors' opinion, it was mainly resulted from the high contributions of the liquid phase particles to the total PN emissions.

Operation parameters of P-N-GPF are shown in Fig. 5. The car running conditions were similar to P-GPF; however, the maximum speed was slightly higher than P-GPF. In addition, P-N-GPF wasn't equipped with any particle removal devices. The overall exhaust temperature was lower than P-GPF, but it was still higher than TWC light-off temperature (approximately 300 °C). Fig. 6 shows NO_x and PN concentration during real-world driving conditions. The trend of the emission concentration was significantly different from P-GPF. Over the rural roads and urban roads, the variations of NO_x concentration from P-N-GPF were lower than P-GPF; additionally, NO_x and PN concentration over motorway was even higher than other road sections. Since P-GPF was equipped with a GPF, PN concentration was at a quite low level, which was significantly different from P-N-GPF. As indicated in Table 1, the compression ratio of P-N-GPF was much higher than P-GPF, leading to the fact that the particle size from P-N-GPF was much smaller than P-GPF theoretically. It was one of the reasons leading to high NO_x emissions for P-N-GPF in the authors' opinion. PN concentration of the petrol cars (Suarez-Bertoa et al., 2019) was much higher than the authors' results that the maximum PN concentration was higher than 3 × 10⁷ #/cm³ (Suarez-Bertoa et al., 2019).

Different from P-GPF and P-N-GPF, D-DPF was a diesel passenger car equipped with a DOC, a DPF, and a SCR. The running parameters of this car are shown in Fig. 7. There weren't many differences among the three cars regarding speed. Because of the low combustion temperature of diesel engines, the exhaust temperature of D-DPF was much lower than P-GPF and P-N-GPF; additionally, the exhaust temperature was dropped below the SCR light-off temperature (180 °C) over several

sections, resulting in low NO_x removal efficiency. The temperature variations during the driving were significant that it was in the range of 140 °C ~ 480 °C. It was mainly caused by the fact that the diesel engine load was mainly controlled by the air/fuel mixture equivalence ratios which had much more impacts on the exhaust temperature than engine speed. Over the sub-urban driving conditions, the exhaust temperature before after-treatment of a diesel passenger car was around 140 °C, with the speed being lower than 40 km/h and frequent start-stop events (Wang et al., 2018). NO_x and PN concentration over the real-world driving is shown in Fig. 8. Over most of the operation conditions, NO_x concentration was at a very low level, except for short periods of large acceleration process and low exhaust temperature sections. PN concentration of this diesel passenger car was much lower than petrol cars that the highest PN concentration was lower than 900 #/cm³. The emission rates of NO_x and PN by travel distance are also provided in Figs. S1–S3.

3.2. Relationships between emissions and driving behaviours

Based on the real-world tests, the average emission rates of NO_x and PN in a small window by the matrix of vehicle speed and acceleration are presented in this section. The intervals of the vehicle speed and acceleration for the window are 2 km/h and 0.1 m/s². Fig. 9 shows NO_x distributions over speed and acceleration. As can be seen, the variations of the acceleration for P-GPF were smaller than the other two cars over the speed range of 25 km/h ~ 40 km/h. It was consistent for the three passenger cars that low NO_x emission rate regions were in the low acceleration (<0 m/s²) and high speed (>30 km/h) regions. Low acceleration process corresponded to small engine torque which

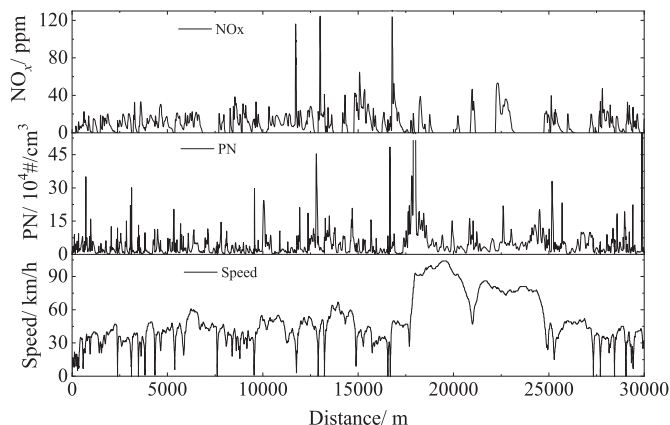


Fig. 6. P-N-GPF emissions over real-world driving conditions.

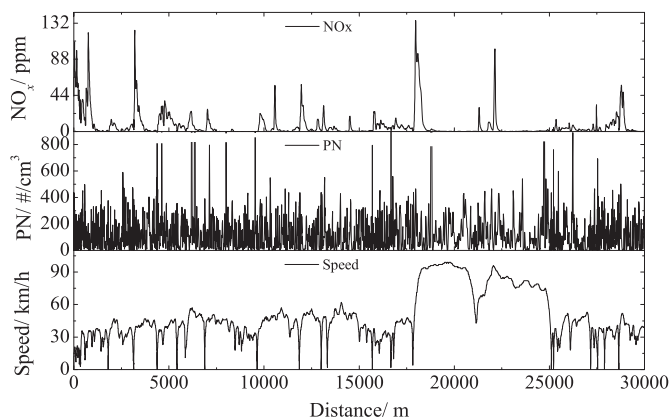


Fig. 8. D-DPF emissions over real-world driving conditions.

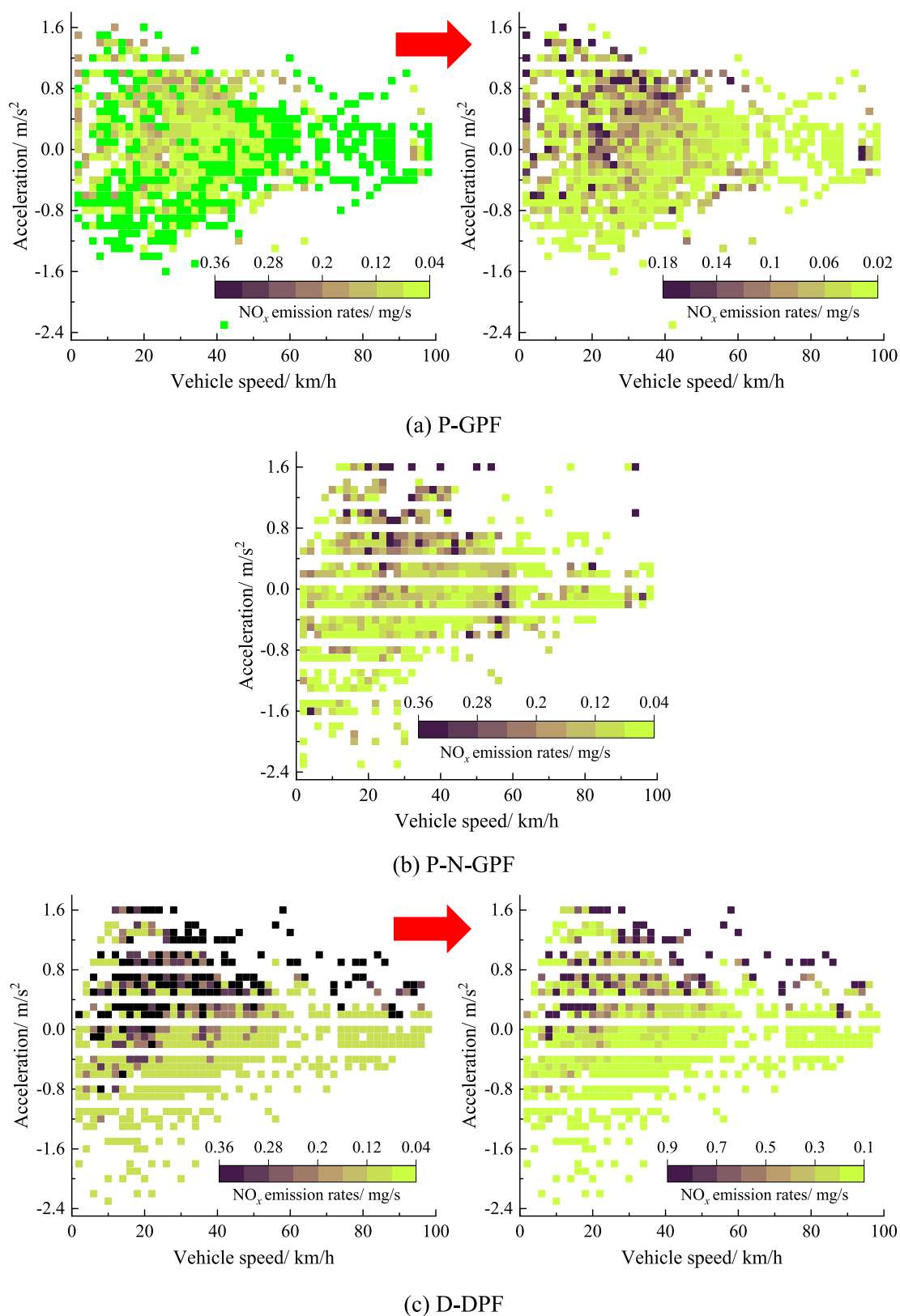


Fig. 9. NO_x distributions over driving behaviours.

led to low in-cylinder combustion temperature theoretically, resulting in a small quantity of NO_x formations. For both petrol cars, high speed (mainly on motorways) delivered very low NO_x emission rates, which resulted from small acceleration and excellent performance of TWCs.

However, it was different for the diesel car which also presented high emission rates over some sections of high speed. In the authors' opinion, it was mainly caused by (1) more NO_x formations due to acceleration; (2) high exhaust temperature which might exceed the

optimal temperature (200–400 °C) of the SCR efficiency. Additionally, it seemed that high emission rates were more dispersive for the petrol cars than the diesel car. It was indicated by Cha et al. (Cha et al., 2019), high NO_x emission rates happened over high speed in urban area and over acceleration process on motorways for a passenger car equipped with a SCR system; however, NO_x emission rates of the one with LNT were high in the whole driving process.

Fig. 10 shows PN distributions over speed and acceleration. For the three passenger cars, variations of PN emission rates were significant;

meantime, high PN emission rates were mainly in the acceleration process and high speed regions. Regarding particles, they included the nucleation mode and accumulation mode. The nucleation mode particles were much smaller than accumulation mode ones, as indicated in the work (Wang et al., 2017). For engine-out PN distributions over particle size, two peaks were usually observed with one corresponding to diameter smaller than 50 nm and the other being in the range of 100–200 nm which were corresponding to the nucleation mode and accumulation mode, respectively (Lin et al., 2021). Regarding GPFs and

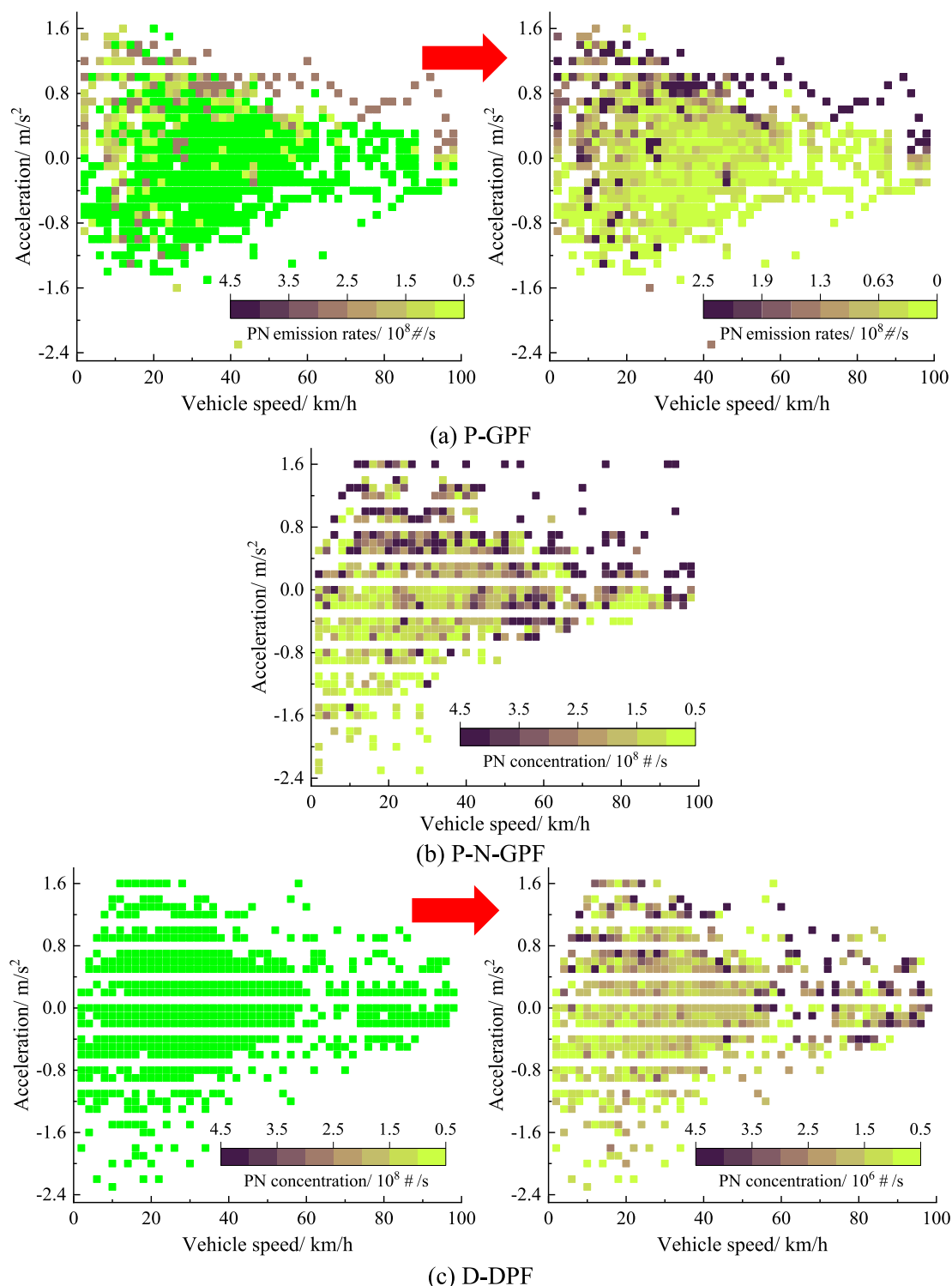


Fig. 10. PN distributions over driving behaviours.

Table 4
Emission factors of the three passenger cars.

	Average speed/km/h	NO _x emission factors/mg/km	PN emission factors/#/km
P-GPF	36.80	3.89	6.8×10^9
P-N-GPF	36.75	7.96	4.2×10^{10}
D-DPF	34.4	18.1	1.4×10^8

DPFs, they were more effective to remove large particles than small ones; meantime, the main ingredients were also different for nucleation mode particles and accumulation mode particles (Reijnders et al., 2018). In addition, the condensations of HC contributed to the increase of nucleation mode particles (Young et al., 2012) which were hard to be captured by GPFs and DPFs. As demonstrated by (Wihersaari et al., 2020) based on a diesel passenger car under deceleration process, the particle size tended to be smaller, and PN emission rates were higher than idle conditions if without DPFs; meantime, the highest PN concentration corresponded to the particle size being smaller than 30 nm. However, the particles size for maximum PN concentration was larger than 30 nm under normal driving conditions (Wihersaari et al., 2020). Most of the particle size was smaller than 50 nm for pipe-out particles with DPF (Wihersaari et al., 2020). In the authors' opinion, the engine-out particles and pipe-out particles for PN distributions were different greatly because of different filter efficiency of GPFs and DPFs for various size particles. PN emission rates were higher than 3×10^{11} #/s for a diesel passenger car without DPF, and they were dropped more than two orders of magnitude after the adoptions of DPF, with the maximum PN emission rates being lower than 10^8 #/s (Wihersaari et al., 2020).

The instantaneous NO_x and PN emission rates are monitored during the test, further the NO_x and PN emission factors can be calculated. The summary of the test results for the three passenger cars is shown in Table 4. The average speed of the three passenger cars was similar. P-GPF presented the lowest NO_x emission factors, and D-DPF had the highest NO_x emission factors. PN emission factors of the diesel passenger car were much lower than the other two petrol cars. P-N-GPF showed the highest PN emission factors. P-N-GPF had a high compression ratio than P-GPF, which led smaller and more particles than P-GPF, which was demonstrated by the work (Di Blasio et al., 2017); additionally, being without GPF also an vital factor causing such a high PN emission factors regarding P-N-GPF between these two petrol passenger cars. The PN emission factors of the P-N-GPF were an order of magnitude higher than P-GPF. The combustion modes of the diesel engine and petrol engine were completely different. Significant fuel rich regions existed in the diesel combustion chamber, which led to larger particle size of diesel engines than the petrol engines. Meantime, the PN emissions greatly depended on the HC emissions which could be condensed into liquid phase particles, leading to more PN emissions. HC emissions of the two petrol passenger cars were much higher than the diesel passenger car, as indicated in Table S1.

Regarding NO_x emissions, low emissions rates were observed under high vehicle speed conditions for all the three cars due to relative small acceleration. The NO_x emission rates were low over low vehicle speed conditions for both petrol passenger cars during the deceleration processes; however, high NO_x emission points were observed under low speed and small deceleration conditions. Due to the limits of the Euro-6 emission regulations on PN emission, GPF is necessary for the gasoline passenger cars to control PN emission; meantime, more attentions should be paid to petrol passenger cars than diesel cars even for the petrol cars equipped with GPF.

4. Discussion

In the real-world driving conditions, vehicle operation conditions are significant factors affecting particle ingredients and numbers. In the

deceleration process, the in-cylinder combustion temperature was low, which led to less solid phase particle formations; low combustion temperature conducted to the formations of liquid phase particles. It was also demonstrated by (Benajes et al., 2017; Xiao et al., 2017), more nucleation mode particles were observed over low engine load conditions. Known from the published papers (Dallmann et al., 2014), the main ingredients of particles from petrol cars and diesel cars differed significantly because of their different combustion modes. Only 5% of the particles in mass were caused by black carbon (solid phase particles) for petrol particles and it was higher than 50% for diesel particles over specific conditions (Dallmann et al., 2014).

Based on the real-world tests of the passenger cars meeting Euro-6 emission standard (including 32 petrol cars and 44 diesel cars in total), NO_x emission factors of 2 petrol cars were higher than Euro-6 limits (Bishop et al., 2019); however, only three diesel cars met the emission regulations, and more than one third of the diesel cars were even higher than Euro-4 emission limits. The test results pointed out the serious problems of NO_x emissions from diesel passenger cars under real-world driving. As for the diesel cars, SCR systems seemed to work much better than lean NO_x trap (LNT) for dropping NO_x emissions (Bishop et al., 2019). Mera et al. (Mera et al., 2019) also compared real-world NO_x emission factors for diesel passenger cars with different NO_x reduction devices. SCR presented much better performance than LNT. Additionally, the real-world NO_x emission factors didn't present much dependency on the car mass, maximum power, and maximum torque (Bishop et al., 2019). More advanced techniques should be used to further drop real-world NO_x emissions, such as electric heated converter (eHC) (Gao et al., 2019a) and ammonia creation and conversion technology (ACCT) (Gao et al., 2021) which work well during cold start stages.

Under the real-world driving conditions, PN emission factors from most of the DI petrol cars without GPFs were beyond the emission limits, which addressed the importance of the GPFs to meet the emission standards (Suarez-Bertoa et al., 2019). Total PN emission factors (1.11×10^{12} #/km) from a DI petrol car were approximately 5 times of the solid phase particles (2.07×10^{11} #/km) (Hu et al., 2021), which indicated that most of the PN from DI petrol cars was contributed by liquid phase particles. Under the same emission standards, PN and PM emission factors from DI petrol cars without GPFs were approximately twice of the ones with GPFs (Hu et al., 2021). McCaffery et al. (McCaffery et al., 2020) also compared PM emissions from DI petrol cars both with and without GPFs, showing that GPFs presented significant reductions in real-world PM emissions. However, the particles being smaller than 23 nm were more than 75% of the total PN for the petrol car with a GPF; and it was 31% for the one without a GPF (Hu et al., 2021). It indicated that GPFs were more effective to control solid phase particles than liquid phase particles. Meantime, PN emissions over cold start were much higher than hot start conditions for the car with GPFs.

Kontses et al. (Kontses et al., 2020) demonstrated that PN emission factors from diesel passenger cars with DPFs were much lower than DI petrol passenger cars without GPFs, which agreed with the authors' results; additionally, the cold start events increased PN emission factors significantly, especially for diesel passenger cars. Platt et al. (Platt et al., 2017) indicated that petrol cars produced more carbonaceous particles than modern filter-equipped diesel cars. Under the urban driving conditions, PN emission factors were much higher than motorways, and the effectiveness of GPFs dropping PN was around 50% (Ko et al., 2019).

5. Conclusions

In this paper, NO_x and PN emissions under real-world driving conditions are monitored using PEMS, and the running parameters of the passenger cars are also recorded. The main conclusions based on the specific passenger cars with given engines are as the follows:

- (1) The driving patterns of the three passenger cars were similar over the given routes, and the speed changed frequently on the rural and urban roads, leading to the frequent changes of car acceleration. The acceleration variations over motorways are low for the three passenger cars.
- (2) Exhaust temperature of both petrol passenger cars was much higher than TWC light-off temperature, especially on the motorways, ensuring the high efficiency of NO_x removal for both petrol passenger cars. Additionally, NO_x concentration was high for rural and motorway driving. Different from both petrol passenger cars, the diesel passenger car presented several high peaks of NO_x concentration, but the NO_x concentration was at a low level in other sections. Maximum PN concentration of the petrol passenger car without a GPF was much higher than the one with a GPF. PN concentration of the passenger cars with a GPF/DPF was much lower than the one without a GPF over motorway.
- (3) NO_x distributions of petrol passenger cars by acceleration and speed were significantly different from the diesel car. Higher PN emission rates of the car without GPF were in a larger region than the car with DPF/GPF. PN emission factors of the petrol passenger car without a GPF were much higher than the other two passenger cars. High compression ratio of the petrol car without a GPF led to small size of particles and high NO_x emission factors than the other petrol passenger cars. Particle size of the diesel passenger car was much larger than both petrol passenger cars.

CRedit authorship contribution statement

Jianbing Gao: Formal analysis, Investigation, Methodology, Resources, Validation, Visualization, Writing - original draft, Writing - review & editing. Haibo Chen: Conceptualization, Funding acquisition, Methodology, Project administration, Resources, Software, Supervision, Visualization, Writing - review & editing. Juhani Laurikko: Data validation, Data collection, Writing - review & editing. Ying Li: Conceptualization, Methodology, Validation, Coordination and Supervision, Writing - review & editing. Ye Liu: Investigation, Writing review & editing.

Declaration of competing interest

The authors declare that they have no known competing financial interests or personal relationships that could have appeared to influence the work reported in this paper.

Acknowledgement

The research reported in this paper was supported by the EU-funded project MODALES (grant agreement No 815189).

Appendix A. Supplementary data

Supplementary data to this article can be found online at <https://doi.org/10.1016/j.scitotenv.2021.149789>.

References

Awad, O.I., Ma, X., Kamil, M., Ali, O.M., Zhang, Z., Shuai, S., 2020. Particulate emissions from gasoline direct injection engines: a review of how current emission regulations are being met by automobile manufacturers. *Sci. Total Environ.* 718, 137302.

Baek, S., Cho, J., Kim, K., Ahn, S., Myung, C.-L., Park, S., 2020. Effect of the metal-foam gasoline particulate filter (GPF) on the vehicle performance in a turbocharged gasoline direct injection vehicle over FTP-75. *Int. J. Automot. Technol.* 21, 1139–1147.

Benajes, J., García, A., Monsalve-Serrano, J., Boronat, V., 2017. An investigation on the particulate number and size distributions over the whole engine map from an optimized combustion strategy combining RCCI and dual-fuel diesel-gasoline. *Energy Convers. Manag.* 140, 98–108.

Bermúdez, V., Luján, J.M., Piqueras, P., Campos, D., 2014. Pollutants emission and particle behavior in a pre-turbo aftertreatment light-duty diesel engine. *Energy* 66, 509–522.

Bielaczyc, P., Woodburn, J., Szczotka, A., 2016. Exhaust emissions of gaseous and solid pollutants measured over the NEDC, FTP-75 and WLTC chassis dynamometer driving cycles. *SAE Technical Paper*.

Bishop, J.D., Molden, N., Boies, A.M., 2019. Using portable emissions measurement systems (PEMS) to derive more accurate estimates of fuel use and nitrogen oxides emissions from modern euro 6 passenger cars under real-world driving conditions. *Appl. Energy* 242, 942–973.

Böttcher, C.F., Müller, M., 2015. Drivers, practices and outcomes of low-carbon operations: approaches of german automotive suppliers to cutting carbon emissions. *Bus. Strateg. Environ.* 24, 477–498.

Cha, J., Lee, J., Chon, M.S., 2019. Evaluation of real driving emissions for euro 6 light-duty diesel vehicles equipped with LNT and SCR on domestic sales in Korea. *Atmos. Environ.* 196, 133–142.

Chan, T.W., Saffaripour, M., Liu, F., Hendren, J., Thomson, K.A., Kubsh, J., et al., 2016. Characterization of real-time particle emissions from a gasoline direct injection vehicle equipped with a catalyzed gasoline particulate filter during filter regeneration. *Emission Control Sci. Technol.* 2, 75–88.

Costagliola, M.A., Costabile, M., Prati, M.V., 2018. Impact of road grade on real driving emissions from two euro 5 diesel vehicles. *Appl. Energy* 231, 586–593.

Dallmann, T.R., Onasch, T.B., Kirchstetter, T.W., Worton, D.R., Fortner, E., Herndon, S., et al., 2014. Characterization of particulate matter emissions from on-road gasoline and diesel vehicles using a soot particle aerosol mass spectrometer. *Atmos. Chem. Phys.* 14, 7585–7599.

Demuyneck, J., Bosteels, D., De Paepe, M., Favre, C., May, J., Verhelst, S., 2012. Recommendations for the new WLTP cycle based on an analysis of vehicle emission measurements on NEDC and CADC. *Energy Policy* 49, 234–242.

Demuyneck, J., Favre, C., Bosteels, D., Hamje, H., Andersson, J., 2017. Real-world emissions measurements of a gasoline direct injection vehicle without and with a gasoline particulate filter. *SAE Technical Paper*.

Di Blasio, G., Belgiorio, G., Beatrice, C., 2017. Effects on performances, emissions and particle size distributions of a dual fuel (methane-diesel) light-duty engine varying the compression ratio. *Appl. Energy* 204, 726–740.

Gao, J., Tian, G., Sornioti, A., 2019a. On the emission reduction through the application of an electrically heated catalyst to a diesel vehicle. *Energy Sci. Eng.* 7, 2383–2397.

Gao, J., Tian, G., Sornioti, A., Karci, A.E., Di Palo, R., 2019b. Review of thermal management of catalytic converters to decrease engine emissions during cold start and warm up. *Appl. Therm. Eng.* 147, 177–187.

Gao, J., Chen, H., Liu, Y., Ying, L., Li, T., Tu, R., et al., 2021. The effect of after-treatment techniques on the correlations between driving behaviours and NO_x emissions of a passenger cars. *J. Clean. Prod.* 288, 125647.

Gao, J., Wang, X., Song, P., Tian, G., Ma, C., 2022. Review of the backfire occurrences and control strategies for port hydrogen injection internal combustion engines. *Fuel*, 121553. In press.

Giechaskiel, B., Joshi, A., Ntziachristos, L., Dilara, P., 2019. European regulatory framework and particulate matter emissions of gasoline light-duty vehicles: a review. *Catalysts* 9, 586.

Hasan, M.A., Frame, D.J., Chapman, R., Archie, K.M., 2019. Emissions from the road transport sector of New Zealand: key drivers and challenges. *Environ. Sci. Pollut. Res.* 26, 23937–23957.

Hays, M.D., Preston, W., George, B.J., George, I.J., Snow, R., Faircloth, J., et al., 2017. Temperature and driving cycle significantly affect carbonaceous gas and particle matter emissions from diesel trucks. *Energy Fuel* 31, 11034–11042.

Hoepfner, A., Roduner, C.A., 2013. PM sensor based on-board diagnosis of particulate filter efficiency. *SAE Technical Paper*.

Hoofman, N., Messagie, M., Van Mierlo, J., Coosemans, T., 2018. A review of the european passenger car regulations—Real driving emissions vs local air quality. *Renew. Sust. Energ. Rev.* 86, 1–21.

Hu, Z., Lu, Z., Song, B., Quan, Y., 2021. Impact of test cycle on mass, number and particle size distribution of particulates emitted from gasoline direct injection vehicles. *Sci. Total Environ.* 762, 143128.

Huang, Y., Surawski, N.C., Organ, B., Zhou, J.L., Tang, O.H., Chan, E.F., 2019. Fuel consumption and emissions performance under real driving: comparison between hybrid and conventional vehicles. *Sci. Total Environ.* 659, 275–282.

Jang, J., Lee, J., Choi, Y., Park, S., 2018. Reduction of particle emissions from gasoline vehicles with direct fuel injection systems using a gasoline particulate filter. *Sci. Total Environ.* 644, 1418–1428.

Karjalainen, P., Pirjola, L., Heikkilä, J., Lähde, T., Tzamkiozis, T., Ntziachristos, L., et al., 2014. Exhaust particles of modern gasoline vehicles: a laboratory and an on-road study. *Atmos. Environ.* 97, 262–270.

Ko, J., Jin, D., Jang, W., Myung, C.-L., Kwon, S., Park, S., 2017. Comparative investigation of NO_x emission characteristics from a euro 6-compliant diesel passenger car over the NEDC and WLTC at various ambient temperatures. *Appl. Energy* 187, 652–662.

Ko, J., Kim, K., Chung, W., Myung, C.-L., Park, S., 2019. Characteristics of on-road particle number (PN) emissions from a GDI vehicle depending on a catalytic stripper (CS) and a metal-foam gasoline particulate filter (GPF). *Fuel* 238, 363–374.

Kontses, A., Triantafyllopoulos, G., Ntziachristos, L., Samaras, Z., 2020. Particle number (PN) emissions from gasoline, diesel, LPG, CNG and hybrid-electric light-duty vehicles under real-world driving conditions. *Atmos. Environ.* 222, 117126.

Lee, W., Schubert, E., Li, Y., Li, S., Bobba, D., Sarlioglu, B., 2016. Overview of electric turbo-charger and supercharger for downsized internal combustion engines. *IEEE Trans. Transp. Electrification* 3, 36–47.

Lelieveld, J., Pöschl, U., 2017. Chemists Can Help to Solve the Air-pollution Health Crisis. *Nature Publishing Group*.

Li, M., Chen, X., Wang, J., Xu, Y., 2013. Study on the PM_{2.5} and ultra fine PM characteristics of diesel vehicle with DPF under the different driving conditions. *Proceedings of the FISITA 2012 World Automotive Congress*. Springer, pp. 779–788.

- Lin, Q., Tay, K.L., Yu, W., Yang, W., Wang, Z., 2021. Effects of polyoxymethylene dimethyl ether 3 (PODE3) addition and injection pressure on combustion performance and particle size distributions in a diesel engine. *Fuel* 283, 119347.
- Marotta, A., Pavlovic, J., Ciuffo, B., Serra, S., Fontaras, G., 2015. Gaseous emissions from light-duty vehicles: moving from NEDC to the new WLTP test procedure. *Environ. Sci. Technol.* 49, 8315–8322.
- McCaffery, C., Zhu, H., Li, C., Durbin, T.D., Johnson, K.C., Jung, H., et al., 2020. On-road gaseous and particulate emissions from GDI vehicles with and without gasoline particulate filters (GPFs) using portable emissions measurement systems (PEMS). *Sci. Total Environ.* 710, 136366.
- Mera, Z., Fonseca, N., López, J.-M., Casanova, J., 2019. Analysis of the high instantaneous NOx emissions from euro 6 diesel passenger cars under real driving conditions. *Appl. Energy* 242, 1074–1089.
- Merkisz, J., Pielecha, J., Bielaczyc, P., Woodburn, J., 2016. Analysis of emission factors in RDE tests as well as in NEDC and WLTC chassis dynamometer tests. *SAE Technical Paper*.
- Merkisz, J., Bielaczyc, P., Pielecha, J., Woodburn, J., 2019. RDE testing of passenger cars: the effect of the cold start on the emissions results. *SAE Technical Paper*.
- O'Driscoll, R., Stettler, M.E., Molden, N., Oxley, T., ApSimon, H.M., 2018. Real world CO2 and NOx emissions from 149 euro 5 and 6 diesel, gasoline and hybrid passenger cars. *Sci. Total Environ.* 621, 282–290.
- Platt, S.M., El Haddad, I., Pieber, S., Zardini, A., Suarez-Bertoa, R., Clairotte, M., et al., 2017. Gasoline cars produce more carbonaceous particulate matter than modern filter-equipped diesel cars. *Sci. Rep.* 7, 1–9.
- Prasath, A., Bernemyr, H., Erlandsson, A., 2020. On the effects of turbocharger on particle number and size distribution in a heavy-duty diesel engine. *SAE Technical Paper*.
- Reijnders, J., Boot, M., de Goey, P., 2018. Particle nucleation-accumulation mode trade-off: a second diesel dilemma? *J. Aerosol Sci.* 124, 95–111.
- Suarez-Bertoa, R., Valverde, V., Clairotte, M., Pavlovic, J., Giechaskiel, B., Franco, V., et al., 2019. On-road emissions of passenger cars beyond the boundary conditions of the real-driving emissions test. *Environ. Res.* 176, 108572.
- Tobías, A., Rivas, I., Reche, C., Alastuey, A., Rodríguez, S., Fernández-Camacho, R., et al., 2018. Short-term effects of ultrafine particles on daily mortality by primary vehicle exhaust versus secondary origin in three spanish cities. *Environ. Int.* 111, 144–151.
- Triantafyllopoulos, G., Dimaratos, A., Ntziachristos, L., Bernard, Y., Dornoff, J., Samaras, Z., 2019. A study on the CO2 and NOx emissions performance of euro 6 diesel vehicles under various chassis dynamometer and on-road conditions including latest regulatory provisions. *Sci. Total Environ.* 666, 337–346.
- Tutuianu, M., Bonnel, P., Ciuffo, B., Haniu, T., Ichikawa, N., Marotta, A., et al., 2015. Development of the world-wide harmonized light duty test cycle (WLTC) and a possible pathway for its introduction in the european legislation. *Transp. Res. Part D Transp. Environ.* 40, 61–75.
- Valverde, V., Mora, B.A., Clairotte, M., Pavlovic, J., Suarez-Bertoa, R., Giechaskiel, B., et al., 2019. Emission factors derived from 13 euro 6b light-duty vehicles based on laboratory and on-road measurements. *Atmosphere* 10, 243.
- Wang, H., Ge, Y., Hao, L., Xu, X., Tan, J., Li, J., et al., 2018. The real driving emission characteristics of light-duty diesel vehicle at various altitudes. *Atmos. Environ.* 191, 126–131.
- Wang, S., Zhu, X., Somers, L., de Goey, L., 2017. Effects of exhaust gas recirculation at various loads on diesel engine performance and exhaust particle size distribution using four blends with a research octane number of 70 and diesel. *Energy Convers. Manag.* 149, 918–927.
- Weber, C., Sundvor, I., Figenbaum, E., 2019. Comparison of regulated emission factors of euro 6 LDV in nordic temperatures and cold start conditions: diesel-and gasoline direct-injection. *Atmos. Environ.* 206, 208–217.
- Wiheraari, H., Pirjola, L., Karjalainen, P., Saukko, E., Kuuluvainen, H., Kulmala, K., et al., 2020. Particulate emissions of a modern diesel passenger car under laboratory and real-world transient driving conditions. *Environ. Pollut.* 265, 114948.
- Xiao, H., Hou, B., Zeng, P., Jiang, A., Hou, X., Liu, J., 2017. Combustion and emission characteristics of diesel engine fueled with 2, 5-dimethylfuran and diesel blends. *Fuel* 192, 53–59.
- Yang, J., Roth, P., Durbin, T.D., Johnson, K.C., Cocker III, D.R., Asa-Awuku, A., et al., 2018. Gasoline particulate filters as an effective tool to reduce particulate and polycyclic aromatic hydrocarbon emissions from gasoline direct injection (GDI) vehicles: a case study with two GDI vehicles. *Environ. Sci. Technol.* 52, 3275–3284.
- Yang, Z., Ge, Y., Thomas, D., Wang, X., Su, S., Li, H., et al., 2019. Real driving particle number (PN) emissions from China-6 compliant PFI and GDI hybrid electrical vehicles. *Atmos. Environ.* 199, 70–79.
- Yinhui, W., Rong, Z., Yanhong, Q., Jianfei, P., Mengren, L., Jianrong, L., et al., 2016. The impact of fuel compositions on the particulate emissions of direct injection gasoline engine. *Fuel* 166, 543–552.
- Young, L.H., Liou, Y.J., Cheng, M.T., Lu, J.H., Yang, H.H., Tsai, Y.I., et al., 2012. Effects of bio-diesel, engine load and diesel particulate filter on nonvolatile particle number size distributions in heavy-duty diesel engine exhaust. *J. Hazard. Mater.* 199, 282–289.